

# DENDROCHEMISTRY AND SOIL CLAY GEOCHEMISTRY APPLIED TO EXPLORATION FOR DEEP U MINERALIZATION AT THE HALLIDAY LAKE PROSPECT, ATHABASCA BASIN, CANADA

P.C.Stewart<sup>1</sup>, T.K.Kyser<sup>2</sup>, L.Lahusen<sup>1</sup>

<sup>1</sup>Uravan Minerals Inc., 2526 Battleford Ave. S.W., Suite 204, Calgary T3E 7J4, Canada ([pstewart@uravanminerals.com](mailto:pstewart@uravanminerals.com)) ([lalahusen@uravanminerals.com](mailto:lalahusen@uravanminerals.com))

<sup>2</sup>Department of Geological Sciences and Engineering, Queen's University, 36 Union St., Kingston K7L 3N6, Canada ([kyser@geol.queensu.ca](mailto:kyser@geol.queensu.ca))

## Introduction

Exploration geologists have a need for innovative geophysical and geochemical remote sensing methods to discover mineralization buried under significant thicknesses of overburden and bedrock because the proportion of near-surface discoveries had decreased dramatically. The Athabasca Basin in northern Saskatchewan, Canada is host to extraordinarily high-grade unconformity-related uranium deposits (e.g. Cigar Lake, McArthur River, at grades >15%). Early discoveries in the basin were made near the surface, (i.e. Rabbit Lake and Key Lake), while more recently discoveries have been made at depths >700 m (ie. Shea Creek and Centennial)(Dahlkamp, 1978; Hoeve and Sibbald, 1978; Laverret et al., 2006; Ceyhan, 2009; Alexandre et al., 2012). The latter two discoveries were made by drill testing deep geophysical targets. The disadvantage of using only geophysical methods to target these deposits is that geophysics is not capable of imaging the U mineralization itself and the geophysical targets are many times larger than the deposit footprint.

Unconformity-related U mineralization is often associated with extensive alteration systems that can be traced from the unconformity to surface. These alterations systems have a distinctive clay mineralogy (typically, illitic, kaolinitic, chloritic or dravitic) and may be enriched in U and pathfinder elements such as Pb, Mo, V, Zn, Ag, Au, Se, S, Bi, Te, Ni, Co, As, Fe and Cu (Sopuck et al., 1983; Hoeve and Quirt, 1984). Deposit related radiogenic Pb can also be subjected to significant lateral and vertical secondary dispersion away from the deposit (Holk et al., 2003). These geochemical characteristics indicate that surface geochemical sampling may be an appropriate way to explore for unconformity-related U mineralization.

The objective of this research is to evaluate whether surface geochemical media can be used to detect geochemical signatures which may originate from unconformity-related U mineralization at significant depths (ca. 750 m). Soil samples and tree cores were collected from the Halliday Lake unconformity-related U prospect. Exploration work on the property to date includes geophysical surveying

and diamond drilling. Geophysical work has identified conductive trends potentially related to graphitic pelitic gneisses, key hosts rocks for unconformity-related U mineralization and sandstone hosted resistivity lows which may be related to hydrothermal clay alteration (Figures 1 and 2) (Hoeve and Quirt, 1984; Powell et al., 2007). Drilling has identified hydrothermal clay alteration, anomalous pathfinder element geochemistry and radiogenic Pb that can be traced from the unconformity to surface (Table 1; Figure 2) (Stewart, 2015). Sub-economic basement hosted U mineralization has also been discovered in a number of drill holes (Table 1; Figure 2). The spatial distribution of radiogenic Pb and the pathfinder elements identified in drill core will be examined in the  $<2\text{ }\mu\text{m}$  clay fraction separated from soil samples and in tree cores with the goal of observing geochemical anomalies that may be related to the underlying bedrock.

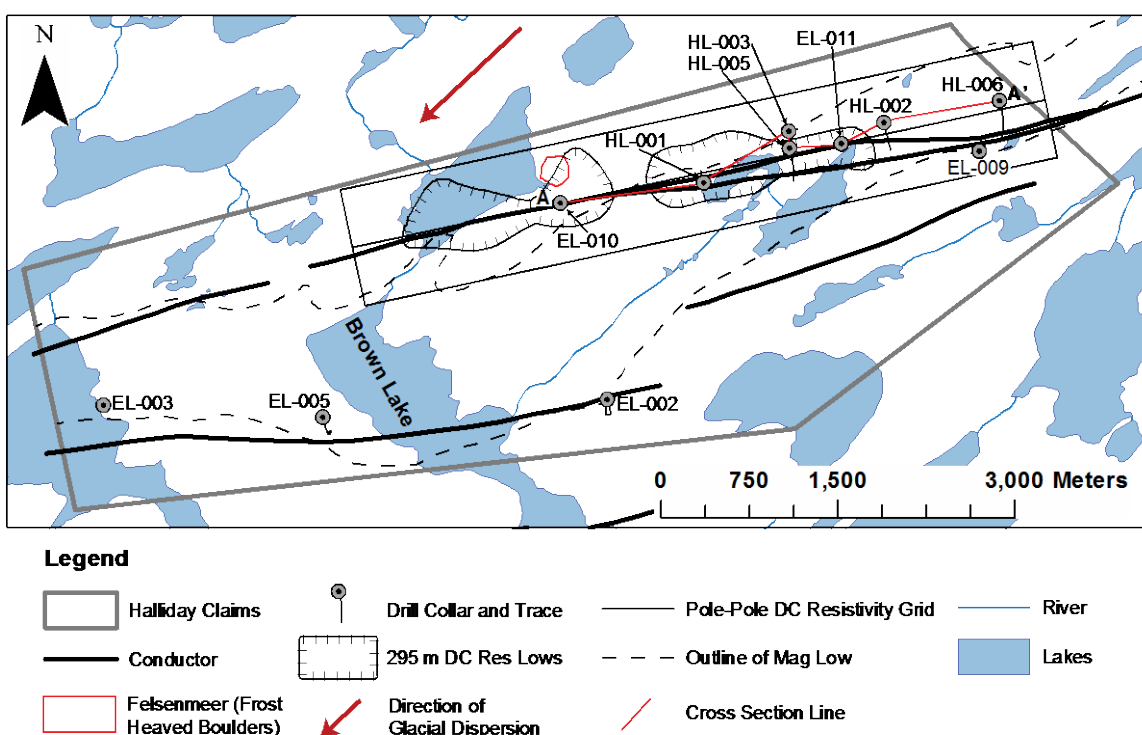


**Figure 1. Map of the Halliday Lake claims showing drill collar locations, the direction of glacial dispersion, location of a felsenmeer boulder field and geophysical features.** The 295 m DC resistivity lows are derived from a 295 m depth slice of an inverted pole-pole DC resistivity survey. The layout of this geophysical survey is shown by the three northeast-southwest trending grid lines. Cross section is A-A' is presented in Figure 2. Azimuth of glacial dispersion is 223° (Schreiner, 1984). Compilation after Uravan Minerals Inc., 2014.

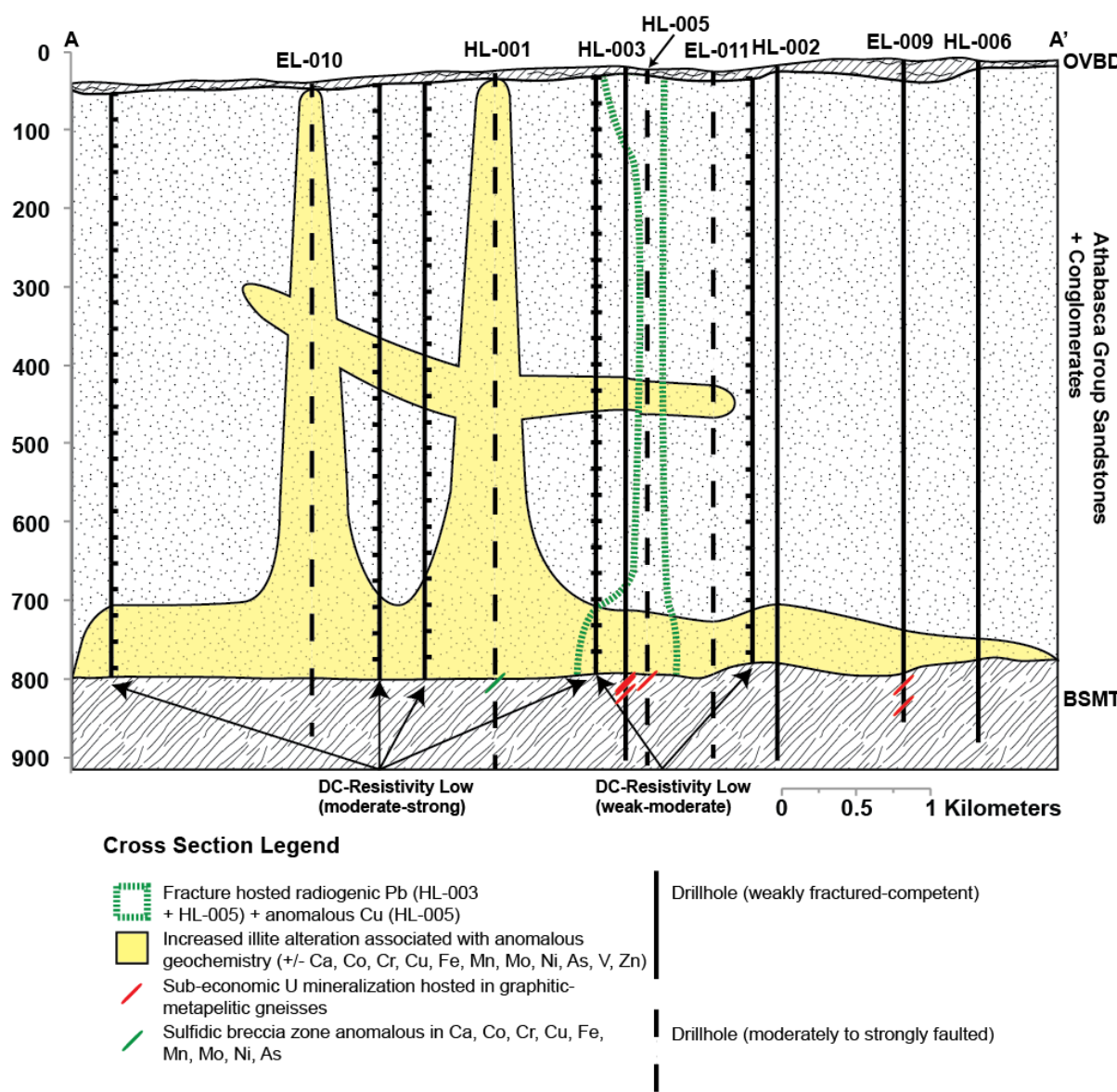


**Figure 2. Schematic cross section A-A' of the northern conductive trend illustrating alteration features, anomalous geochemistry, sub-economic U mineralization and the extent of the sandstone hosted resistivity lows. OVBD and BSMT represent overburden and basement respectively. See Figure 1 for cross section layout.**

**Table 1. Summary of drilling results at the Halliday Lake prospect.** All uranium mineralization reported is hosted in graphitic metapelites. Basement rocks are listed in order of highest to lowest abundance within a given drill hole (Stewart, 2015).

DDH	OVBDN	UC	SST	EOH	mASL	Basement Rocks Structure	Alteration	Geochemistry	U Mineralization	Pb Isotopes	
HL-001	11	775	784	800	574	Psammite, calc-silicate, graphitic metapelites	Common moderate to strong fracturing 200 m to UC, sulfide fracture zone immediately below UC	Dominant illite +/- chlorite, dravite throughout, subhedral quartz in SST and BSMT near UC	SST: enriched throughout in Ca, Co, Cr, Cu, Fe, Mn, Mo, Ni associated with fracturing, U enrichment within 50 m of UC, BSMT sulfide fault enriched Ca, Co, Cr, Cu, Fe, Mn, Mo, Ni, U, BSMT U enrichment within ~8 m of UC	-	Radiogenic features isotopes from 525 m to the UC
HL-002	8	785	768	800	582	Graphitic metapselite, calc-silicate, pegmatite	Rare SST hosted fracturing, 3 graphitic BSMT hosted faults	Illite +/- chlorite dravite in Mfa	Weak SST enrichment with 60 m of the UC of U, Cu, Co, BSMT U enrichment within ~5 m of the UC	-	Radiogenic Pb features from 815 m to the UC
HL-003	8	774	788	807	583	Pegmatite, graphitic metapelites	Moderate fracturing upper ~400 m, subhorizontal pegmatite hosted fracturing	Weak illite +/- chlorite, dravite in Mfo, illite +/- chlorite dravite in Mfa	Enriched in Ca, Co, Cr, Cu, Fe, Mn, Mo, Ni in association with increased illite alteration in Mfo, BSMT U enrichment within ~15 m of the UC	177.1 ppm (0.3), 188.4 ppm (0.3), 188.1 (0.16)	Radiogenic Pb features from 700 m to the UC and also from surface to ~125 m
HL-005	8	772	784	807	577	Graphitic metapselite, pegmatite	Moderate fracturing throughout, subhedral quartz observed on fracture faces in SST and BSMT	Illite +/- chlorite, dravite in Mfo, Mfa, subhedral quartz in SST and BSMT, kaolinite near surface	Enriched in Cu, Ca, Co, Fe, Mn in fractured intervals and in association with increased illite alteration in the Mfo, BSMT U enrichment within ~3 m of the UC	732.6 ppm (0.26), 232 ppm (0.1)	Radiogenic features from ~125 m to the UC
HL-006	11	788	765	871	588	Pegmatite, graphitic metapselite	Weak fracturing in Mfd, Mfb, brittle healed fault hosted in graphitic metapselite	Moderate-weak illite +/- chlorite, dravite in Mfa	Enrichment in Cu, Mo in Mfa and near UC	-	Radiogenic features from 715 to UC, from surface to 80 m
EL-002	17	789	788	803	578	Graphitic metapselite, pegmatite	Common moderate to strong fracturing from surface to UC, 3 basement hosted graphite to chlorite faults	Subhedral quartz in fractures below ~650 m	ND	ND	ND
EL-003	13	780	787	877	586	Calc-silicate, pegmatite, graphitic metapselite	Minor sporadic fracturing below ~600 m	ND	ND	ND	ND
EL-005	80.4	823	743	878	573	Graphitic metapselite, pegmatite	~10 m scale fracture zones near base of Mfd and Mfa	ND	ND	ND	ND

DDH: diamond drill hole    OVBDN: overburden thickness (m)    UC: unconformity depth (m)    SST: sandstone thickness (m)    EOH: end of hole (m)  
 mASL: collar elevation above sea level    ND: no data available    -: no significant U mineralization

DDH	OVDN	UC	SST	EOH	mASL	Basement Rocks Structure	Alteration	Geochemistry	U Mineralization	Pb Isotopes
EL-008	27	785	788	846	688	Pegmatite, graphitic metapselite	Rare sandstone hosted fracturing, graphitic BSMT hosted fault	Weak illite +/- chlorite in Mts	Basement hosted B enrichment (>1000 ppm over ~40 m)	1026 ppm (0.5 m), 1180 ppm (0.1 m, pitchblende on fracture face)
EL-010	6.6	782	788	846	682	Pegmatite, calc-silicate, graphitic metapselite	Common moderate to strong fracturing present from ~127 m to UC, 2 graphitic and sulfide fault zones	Dominant illite +/- davrite, chlorite throughout, euhedral quartz	SST enriched throughout in As, Zn, MnO, CaO, Pb, MgO, and K2O, below 460 m to the UC enriched in Cu, Ni, V and B associated with fracturing, U enrichment near UC BSMT U enrichment within 8 m of the UC	-
EL-011	10.0	772	781	878	678	Pegmatite, calc-silicate gneiss (trace graphite)	Sporadic weak to moderate fracturing throughout the sandstone, subhorizontal pegmatite hosted fracturing	Illite in MFC, moderate illite +/- chlorite in Mts	Weak Pb enrichment at ~400 m	-

DDH: diamond drill hole    OVDN: overburden thickness (m)    UC: unconformity depth (m)    SST: sandstone thickness (m)    EOH: end of hole (m)  
 mASL: collar elevation above sea level    ND: no data available    -: no significant U mineralization

## Methodology

Tree core and soil samples were collected from the Halliday Lake unconformity-related U prospect over two sampling programs, which ran in June 2011 and July 2012. The initial program collected samples from 307 sites using a 250 m offset grid spacing. The second sampling grid consisted of 161 sample sites over an area which was identified as anomalous in 2011. This grid was offset from the 2011 grid and was also collected at an offset grid spacing of ~250 m, giving the area an effective grid spacing of ~125 m.

### Sampling Methodology

Tree cores were collected from mature (>6 cm diameter) black spruce (*Picea mariana*) and jack pine (*Pinus banksiana*) trees, where available. At sample sites where both black spruce and jack pine trees are present, black spruce were the preferred sample media, as biogeochemical work in the Athabasca Basin by Dunn (1981) indicates that this species is effective at recording U over areas of U mineralization. Tree cores were collected using a 14 inch long, 5.15 mm steel increment bore. This bore was drilled through the center of the tree in a north-south orientation, and the resultant core was placed into a drinking straw and sealed with packing tape. The sample number and orientation were identified on the straw.

In the temperate, conifer-dominated boreal forest of northern Saskatchewan, the dominant soil type is podzol (Rose et al., 1979). Podzols can be broken down into three basic soil horizons from surface to bedrock: A, B and C. Soil samples at Halliday Lake were collected from the C horizon where possible, and from a horizon informally referred to as the B2 horizon (lower B horizon) in areas where the C horizon was not encountered. The upper B soil horizon (informally referred to as the B1 horizon) is distinguished from the overlying A and the underlying C soil horizons by its characteristic red-brown colour. The colour is related to an increased proportion of Fe-Mn oxides and elevated clay content relative to the eluviated overlying A soil horizon. The B2 soil horizon occurs as a bleached horizon below the red-brown Fe-Mn oxide-rich B1 horizon, and has lower clay content relative to the underlying C soil horizon. The C soil horizon is also bleached relative to the overlying B1 horizon, but is richer in finer grained material relative to the B2 soil horizon, and is composed of variably weathered till and bedrock material. Samples were collected from holes dug with a stainless steel spade to a depth between ~0.5-1.0 m to collect the C, B2 or rarely (where digging conditions are prohibitive) B1 soil horizon. One kilogram of sample was collected for each sample site and was placed into a double zipper plastic bag, labeled with the sample number and specific horizon from which the sample was taken.

## Sample Preparation and Analytical Methodology

Tree core samples were prepared and analyzed at the Queen's Facility for Isotope Research (QFIR), Kingston, Ontario. Each of the tree rings was counted thus giving the age of the tree, and any variability in ring widths was noted. Where tree age permitted, segments were collected between or before the years of 1970-1985, prior to significant mining and development activity in the Athabasca Basin; in younger trees, the oldest intervals were selected. However, in all cases, care was taken not to select segments from the sapwood, as the chemistry within these portions of the trees can be quite variable (Cutter and Guyette, 1993). Selected tree ring segments spanning about 5 years were kept at a consistent length (approx. 1cm) to ensure consistent analytical results. Sampled segments were cleaned in deionized water (18.2 MΩ resistivity) in an ultrasonic bath for 10 min before being dried at 70°C overnight. Once dried, selected intervals were digested using a Teflon-tube microwave system in which 4 mL of distilled concentrated nitric acid and 2 mL of 30% ultra-pure hydrogen peroxide were added to each sample and heated to 200°C for approximately 20 min. Digested samples were dried at 70°C on a hotplate in a fumehood in a class 100 clean lab, and diluted to 8 mL using 2% nitric acid spiked with In as an internal standard.

Lead isotopes and trace elements (50) were measured in tree core solutions using a Thermo Scientific Element 2 XR HR-ICP-MS and major elements were analyzed, using a Thermo Scientific iCAP ICP-OES. The NIST1547 peach leaf certified reference material (CRM) and two in-house standards (black spruce bark and twigs) were used as matrix-matched reference materials. The NIST981 and NIST983 CRMs, (common and radiogenic Pb isotope standards, respectively), were also used to monitor instrumental drift. Mass bias for Pb isotopes was corrected using solutions spiked with Ti. Procedure blanks were run every 14 samples. Intensities for all elements were blank subtracted, and <sup>202</sup>Hg intensities were used to corrected <sup>204</sup>Hg and <sup>204</sup>Pb interference.

The <2 µm clay fraction was separated from the soils at QFIR. The <2 µm clay fractions are potentially ideal soil sampling media because their surfaces are highly charged and act as sites to adsorb trace metals and preserve anomalous isotope ratios dispersed from a deposit at depth (Shilts, 1995). Approximately 300 mL of soil was sieved to remove pebbles and any large organic material before adding ~700 mL of reverse osmosis (RO) water and a spoonful of Calgon® (sodium meta-hexamphosphate). The Calgon® is a deflocculant used to increase the proportion of clay content yielded from a given sample. This mixture was then agitated for 120 seconds using an ultrasonic probe. Two centrifuge steps for 30 seconds at 2000 rpm and 120 seconds at 8000 rpm are used to separate the >2 µm and <2 µm clay fractions respectively. The >2 µm fraction is discarded whereas the <2 µm clay fraction is dried in an oven at 70° C before being weighed and placed in a plastic sample bag. Replicates of samples were completed and submitted every 60 samples to ensure reproducibility. The <2 µm clay fraction was submitted to ACME labs in

Vancouver, British Columbia, Canada, and analyzed by ACME's 1F ultratrace *aqua regia* digestion. Samples were analyzed for 53 elements, REEs, and Pb isotopes by ICP-MS.

## Results

### Dendrochemistry

Different tree species may respond differently to different trace metals; therefore a comparison of the jack pine and black spruce tree core results is necessary to identify those elements whose median concentrations are significantly different, ca. >60% (Table 2). Chromium, and Mo concentrations differ significantly between black spruce and jack pine trees, and as such only the black spruce results will be presented for these elements.

**Table 2. Summary statistics of key elements and Pb isotope ratios for jack pine and black spruce trees.** Count represents the number of samples that gave results above detection limits. Those elements for which the median values of jack pine and black spruce trees differed by more than 60% are bolded.

Element/Ratio	Black spruce				Jack pine				Count
	Median	Max	Min	Count	Median	Max	Min	Count	
$^{207}\text{Pb}/^{206}\text{Pb}$	0.838	0.891	0.403	231	0.819	0.867	0.570	77	
Co ppb	12.4	129.7	3.0	223	14.0	154.1	4.7	77	
Cr ppm	<b>0.7599</b>	<b>5.1019</b>	<b>0.0939</b>	<b>231</b>	<b>0.3934</b>	<b>12.2354</b>	<b>0.1096</b>	<b>76</b>	
Cu ppm	0.5443	1.8724	0.2575	230	0.4688	1.3018	0.2292	77	
Fe ppm	14.761	316.352	2.554	231	9.892	386.923	2.422	77	
Mo ppb	<b>62</b>	<b>803</b>	<b>8</b>	<b>231</b>	<b>32</b>	<b>956</b>	<b>3</b>	<b>75</b>	
Ni ppm	0.311	2.270	0.037	231	0.241	4.735	0.076	77	
Pb ppb	27.05	363.25	4.81	231	19.60	117.86	8.17	77	
S ppm	43.68	95.97	21.37	230	41.97	72.47	20.30	77	
U ppb	0.87	115.16	0.28	230	1.20	50.24	0.36	76	

In Figure 3, contour maps of U, Pb, Mo, S, Co, and Cu concentrations in tree core samples are presented. Uranium is the commodity of interest, while Pb, Mo, S, Co, and Cu are pathfinder elements for unconformity-related U deposits. Uranium concentrations peak west to northwest of Brown Lake, with the highest concentrations located north and south of a break in the northern conductor. Higher concentrations are also present near the northern and southern trace of the magnetic low in the eastern portion of the prospect and directly east of Brown Lake, south of the western resistivity low. Lead concentrations are highest west of the Brown Lake and west of the break in the northern conductor and north of the western resistivity low. Molybdenum concentrations are highest north of Brown Lake and are associated with a bend in the magnetic low, near the southern portion of Brown Lake where the river drains into it and northwest of the break in the northern conductor. Sulfur concentrations are elevated between the two resistivity lows, associated with the river draining into the southern part of Brown Lake, and west of Brown Lake

associated with the southwest conductor. Cobalt and Cu concentrations are elevated in association with sandstone boulders near the river that runs from the northwest of Brown Lake, and with the felsenmeer boulders.

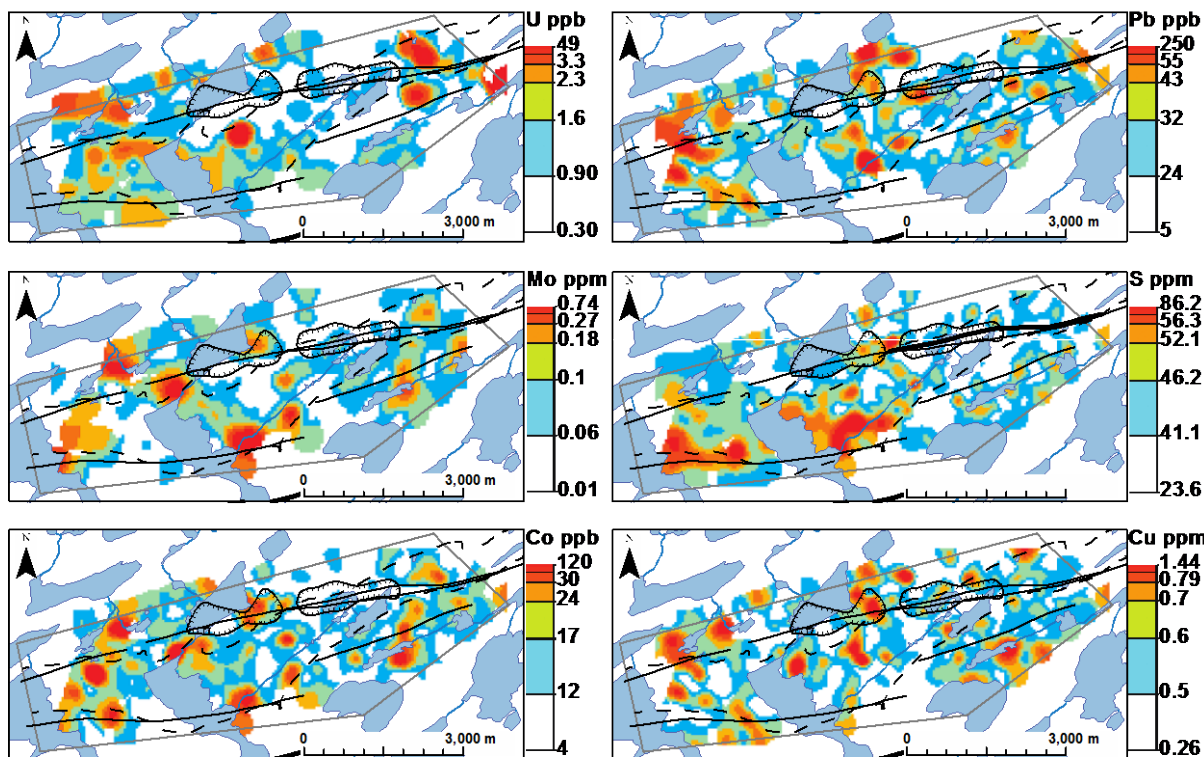


**Figure 3. Contour plots of U, Pb, Mo, S, Co, and Cu concentrations for tree cores. The elements Ni, Cr, and Fe, exhibit similar trends to those shown by Co. See Figure 1 for a geophysical and physiographic legend.**

### <2 µm Clay Fraction Geochemistry

The elements of interest in the <2 µm clay fraction include U, Pb, Al, Mg, As and Mo, with the spatial distribution of Co, Mn, Rb, Ni, K, Cu, Ca, Bi, Ba, Cr, Cs, and Li being nearly identical to that of Mg (Figure 4). Uranium is the commodity of interest, Mg is associated with hydrothermal clay alteration, and As and Mo are pathfinder elements and aluminum may be representative of the proportion of clay in a sample. Uranium concentrations are elevated at the eastern edge of the eastern resistivity low, between the two resistivity lows, and south of the western resistivity low. Lead concentrations show a strong cluster of anomalous east of Brown Lake, and to the southeast of the resistivity low. Elevated Pb concentrations are present northeast of the resistivity low. Aluminum concentrations are elevated to the west of Brown Lake, and between a break in the southern conductive trend. Magnesium concentrations are elevated east of Brown Lake coincident with, and to the south of the northern conductor. There is a relatively prominent northwest-southeast trend of elevated Mg concentrations that begins south of the western resistivity low, terminates at the break in the southern conductor. Arsenic concentrations are elevated at the western edge of the prospect, at the break in the southern conductor,

and north of the split northern conductor. Molybdenum concentrations are elevated coincident with, and southwest of, the western resistivity low, in the central eastern portion of the prospect, and south of the break in the southern conductor.

**Table 3. Summary statistics of key elements and Pb isotope ratios from the <2 µm clay fraction. Count represents the number of samples that gave results above detection limits.**

Element/Ratio	Median	Max	Min	Count
$^{207}\text{Pb}/^{206}\text{Pb}$	0.633	0.876	0.401	382
As ppm	6.6	14.7	0.3	382
Al %	7.29	10	0.82	382
Ba ppm	151	385	31	382
Bi ppm	0.85	4.09	0.18	382
Ca %	0.1	0.3	0.02	382
Co ppm	9.5	40.3	0.7	382
Cr ppm	62	230	12	382
Cs ppm	3.76	13.4	0.63	382
Cu ppm	15.70	70.17	3.15	382
K %	0.13	0.65	0.03	382
La ppm	19	108	5	382
Li ppm	40.9	107.8	1.4	382
Mg %	0.5	1.87	0.03	382
Mn ppm	180.5	1442	13	382
Mo ppm	1.2	3.85	0.21	382
Nd ppm	15.34	101.76	4.69	382
Ni ppm	21.9	71.2	3.5	382
Pb ppm	21.14	85.27	4.43	382
Th ppm	14.43	58.357	0.008	382
U ppm	1.879	7.294	0.636	382
V ppm	92	289	8	382

### Pb Isotope Ratios

Low  $^{207}\text{Pb}/^{206}\text{Pb}$  ratios can reflect Pb derived from the decay of U and as such, may be useful for vectoring to unconformity-related U deposits in the surficial environment (e.g. Holk et al., 2003). Changes in the slope of probability plots of  $^{207}\text{Pb}/^{206}\text{Pb}$  ratios from tree cores (Figure 5A) and <2 µm clay separates (Figure 5B) identify two possible populations of anomalously low (radiogenic)  $^{207}\text{Pb}/^{206}\text{Pb}$  ratios for each of the media. For tree cores, the breaks occur at  $^{207}\text{Pb}/^{206}\text{Pb}$  ratios of 0.670 and 0.798, whereas for the <2 µm clay fraction they occur at 0.540 and 0.578.

The spatial distribution of the anomalous  $^{207}\text{Pb}/^{206}\text{Pb}$  ratios in tree cores and clay fraction samples is presented in Figure 5. There are no clusters of the most radiogenic tree cores ( $^{207}\text{Pb}/^{206}\text{Pb}$  ratios <0.67). The second population of radiogenic tree cores ( $^{207}\text{Pb}/^{206}\text{Pb}$  ratios <0.798) forms two clusters; one on the northern edge of the claims and one cluster near the southern edge. In the central portion of the prospect, there is an east-west trend of radiogenic tree cores associated with the edge of the magnetic low towards the west end and persists to north of the

conductor. Radiogenic tree cores are also sporadically associated with the southern conductive trends and with the split in the northern conductive trend.

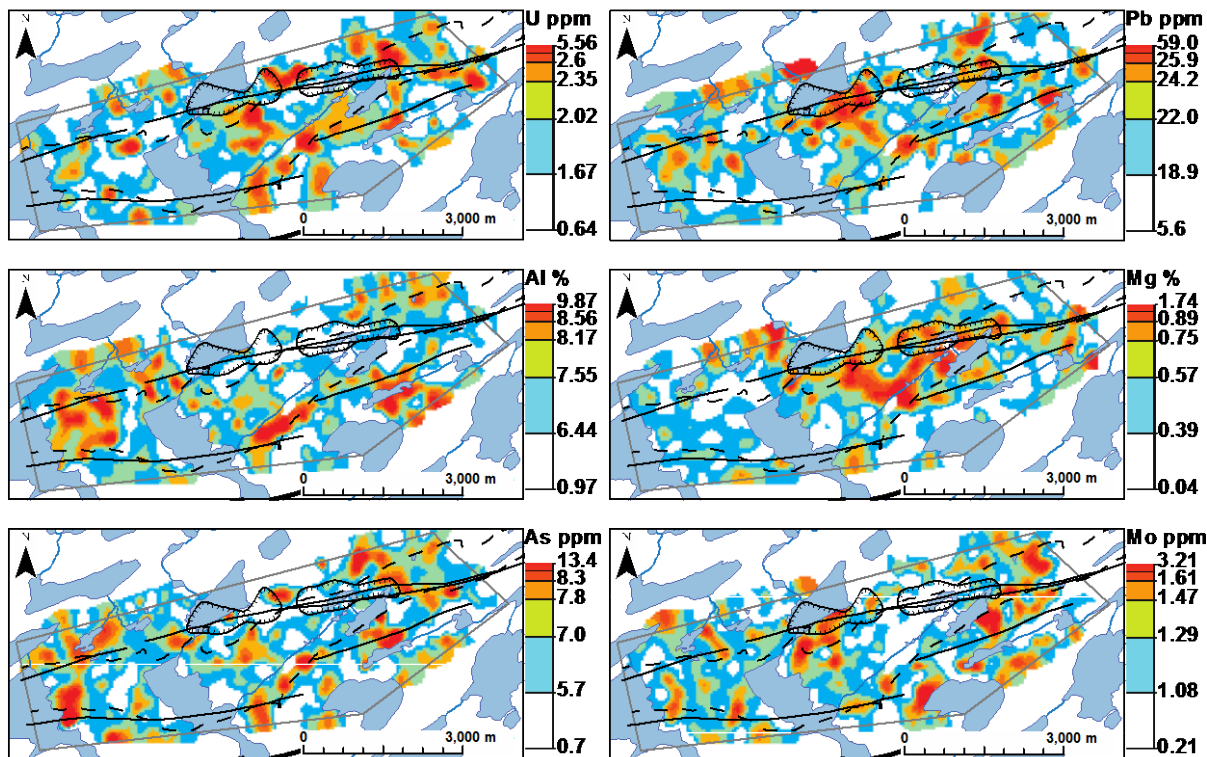


**Figure 4. Contour plots of U, Pb, Al, Mg, As and Mo for <2  $\mu\text{m}$  clay fraction. Similar trends to those of Mg are exhibited by Co, Mn, Rb, Ni, K, Cu, Ca, Bi, Ba, Cr, Cs, and Li. See Figure 1 for a geophysical and physiographic legend and drill hole labels.**

A number of clusters of radiogenic <2  $\mu\text{m}$  clay fraction samples are present east of Brown Lake (Figure 5D). The most prominent cluster is immediately east of Brown Lake, has a northwest-southeast trend, and is composed of samples from both populations identified in Figure 5B. Much of this cluster is spatially associated with the conductor trace, the DC-resistivity low, and the warp in the edge of the magnetic low. There are also a few minor clusters present along the trend of the eastern portion of the southern conductor. Finally, there are some radiogenic clusters associated with the location of weakly U mineralized drill holes HL-003, HL-005, and EL-009.

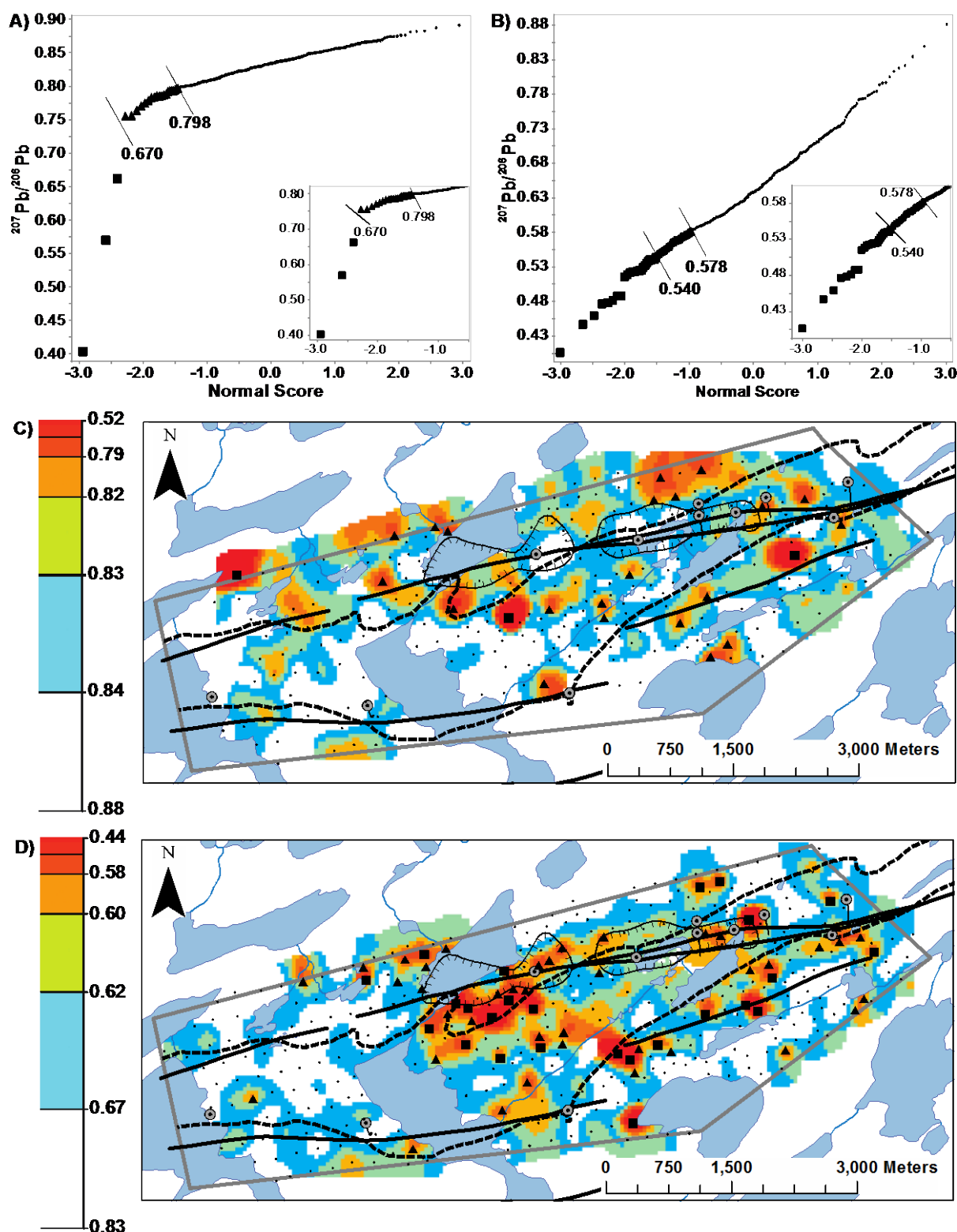


**Figure 5. Normal probability plots of  $^{207}\text{Pb}/^{206}\text{Pb}$  ratios for trees cores (A) and <2  $\mu\text{m}$  clay fractions (B).** Samples with anomalous ratios are defined by breaks in the slope of the normal probability plot and are represented by squares (most anomalous), and triangles (secondary population). Maps C) and D) are the spatial distribution of anomalous  $^{207}\text{Pb}/^{206}\text{Pb}$  isotope ratios for tree cores and <2  $\mu\text{m}$  clay fractions as defined in (A) and (B). See Figure 1 for physiographic and geophysical legend and drill hole labels.

## Discussion

While no unconformity-related U deposit has yet been discovered at the Halliday Lake prospect, both geophysical data and diamond drilling have identified favourable features. Areas of increased faulting, hydrothermal alteration and anomalous geochemistry are associated with the DC resistivity low, indicating that this resistivity low is associated with these positive geological features (i.e. drill holes EL-010, EL-011, HL-001, HL-005, see Table 1; Figures 1 and 2). Holes EL-009, HL-003 and HL-005 are host to sub-economic basement U mineralization, and the latter two drill holes have radiogenic Pb near the surface (Table 1; Figure 2). These features indicate that geochemical anomalies should be present east of Brown Lake, in association with the northern conductor and the resistivity lows, and potentially locally in association with EL-009.

The <2 µm clay fraction map of Mg concentrations in Figure 4 shows that elevated concentrations are spatially associated with the eastern resistivity low where HL-001 is located. This anomalous trend of Mg concentrations also correlates with anomalies in a number of elements including Co, Cu, and Mn, which were also anomalous in drillholes HL-001 and HL-005 (Table 1). Mineralized holes HL-003 and HL-005 are also associated with elevated Pb concentrations and radiogenic Pb in the <2 µm clay fraction. Thus in this area the <2 µm clay separates appears relatable to the underlying bedrock geochemistry.

The length of the western resistivity low is highlighted by radiogenic  $^{207}\text{Pb}/^{206}\text{Pb}$  ratios and elevated Pb and Mo concentrations in the <2 µm clay fraction (Figures 4 and 5). Elevated tree core concentrations of Pb, Mo, S, Co, and Cu are present at the eastern end and in some instances north of the resistivity low (Figure 3). This area highlighted by the tree cores is directly coincident with EL-010 and also with a field of felsenmeer boulders (Figure 1). Drill hole EL-010 is associated with anomalous geochemistry, faulting, and alteration and thus the surface geochemical anomalies detected in the tree cores and the <2 µm clay fractions may be related to the underlying bedrock (Table 1).

Near drill hole EL-009 along the conductive trend a number of anomalous geochemical features are observed. Radiogenic  $^{207}\text{Pb}/^{206}\text{Pb}$  ratios, elevated As, Mo and U concentrations are present in the <2 µm clay fraction, while elevated U concentrations and radiogenic  $^{207}\text{Pb}/^{206}\text{Pb}$  ratios are also present in the tree cores (Figures 3, 4 and 5). Whilst drill hole EL-009 is not associated with significant alteration or geochemical anomalies, it is host to two U mineralized intercepts hosted in graphitic-metapelitic gneisses (Table 1).

The above discussion demonstrates that surficial geochemical anomalies do appear to be related to anomalies in drilling results, geophysics and physiography, although there are a few differences. For example enrichments in the <2 µm clay fraction pathfinder elements such as Mg, Cu, Co and Mn appear to be conformable

to known anomalous bedrock as defined by drilling and geophysics (Figure 4). Molybdenum's behaviour is in contrast with these elements (Figure 4). Molybdenum concentrations are known to be elevated in drill hole HL-001 (Table 1). However, in the <2 µm clay fraction, Mo concentrations are not directly coincident with HL-001, which may suggest that glacial dispersion to the southwest has physically displaced the Mo anomalies from the potential bedrock source in HL-001.

Biogeochemical anomalies associated with the northern conductor are less extensive than that recorded by the <2 µm clay fraction and are generally restricted to the vicinity of the geochemically anomalous drill hole EL-010 and the western resistivity low (Table 1; Figure 3). The anomalous element assemblage of Pb, Mo, S, Co and Cu present in the area is particularly compelling, as unconformity-related U deposits can be associated with significant base metal enrichment related to sulfide and arsenide mineralization (Hoeve and Quirt, 1984). This area is associated with *in situ* frost heaved bedrock (*felsenmeer*) and therefore anomalies that formed here are likely representative of the immediately underlying bedrock (Figure 1). Therefore the tree cores are likely reflecting the anomalous bedrock geochemistry known to be present in drill hole EL-010.

The <2 µm clay fraction  $^{207}\text{Pb}/^{206}\text{Pb}$  ratios are radiogenic in areas where mineralization has been intercepted by drilling (e.g. HL-003, HL-005, EL-009) and are generally non-radiogenic in areas where no mineralization has been intercepted (e.g. HL-001, HL-006, EL-002, EL-005, EL-006) (Figure 5; Table 1). This is supported by the radiogenic  $^{207}\text{Pb}/^{206}\text{Pb}$  ratios near surface in both HL-003 and HL-005 (Stewart, 2015). There are some radiogenic  $^{207}\text{Pb}/^{206}\text{Pb}$  samples near HL-002 and EL-011 (non-mineralized holes), however these appear to be point anomalies. Hole EL-010 is associated with radiogenic  $^{207}\text{Pb}/^{206}\text{Pb}$  ratios without any associated U mineralization; however, a relatively thick section of U enrichment is present within the basement (Table 1).

## Conclusions

The <2 µm clay fraction geochemistry and the tree core biogeochemistry correlate well with known alteration, geochemical anomalies and sub-economic U mineralization in the Athabasca Group and basement rocks. An area that was already known to be anomalous (EL-010) from drill core was highlighted by Pb, Co, etc. in both media.

In the <2 µm clay fractions anomalous Mg, Mn, Co and Cu concentrations are conformable to known geological features whereas elements such as Mo appear to be glacially dispersed from their bedrock source. Radiogenic Pb detected in the <2 µm clay fraction in particular appears to be a very powerful tool for delineating potential areas of U mineralization.

Tree core biogeochemical anomalies in this area are more localized, however they can be related directly to known anomalous geochemistry present in EL-010

due to the minimal overburden in the area. This significantly enhances the robustness of these anomalies.

Overall the geochemical anomalies recorded in both <2 µm clay separates and tree cores suggest that the potential for the Halliday Lake prospect to host U mineralization is high. Follow up drilling should be focused in areas where the <2 µm clay fraction identified radiogenic Pb isotopes in proximity to multi-element anomalies recorded in both the <2 µm clay separates and the tree cores.

## References

- ALEXANDRE, P., KYSER, K., JIRICKA, D. AND WITT, G. 2012. Formation and evolution of the Centennial unconformity-related uranium deposit in the South-Central Athabasca Basin, Canada. *Economic Geology* **107**:385-400.
- CEYHAN, M. 2009. World distribution of uranium deposits (UDEPO) with uranium deposit classification. *International Atomic Energy Agency*, IAEATECDOC-1629.
- CUTTER, B.E. and GUYETTE, R.P. 1993. Anatomical, chemical, and ecological factors affecting tree species choice in dendrochemistry studies. *Journal of Environmental Quality* **22**:611-619.
- DALHKAMP, F.J. 1978. Geologic appraisal of the Key Lake U-Ni deposits, northern Saskatchewan. *Economic Geology* **73**:1430-1449.
- DUNN, C.E. 1981. The biogeochemical expression of deeply buried uranium mineralization in Saskatchewan, Canada. *Journal of Geochemical Exploration* **15**:437-452.
- HOEVE, J. & QUIRT, D. 1984. Mineralization and host rock alteration in relation to clay mineral diagenesis and evolution of the Middle-Proterozoic, Athabasca Basin, Northern Saskatchewan, Canada. Saskatchewan Research Council Technical Report No. 187.
- HOEVE, J. & SIBBALD, T.I. 1978. On the genesis of Rabbit Lake and other unconformity-type uranium deposits in northern Saskatchewan, Canada. *Economic Geology* **73**:1450-1473.
- HOLK, G.J., KYSER, T.K., CHIPLEY, D., HIATT, E.E. and MARLATT, J. 2003. Mobile Pb-isotopes in Proterozoic sedimentary basins as guides for exploration of uranium deposits. *Journal of Geochemical Exploration*, **80**:297-320.
- LAVERRET, E., MAS, P.P., BEAUFORT, D., KISTER, P., QUIRT, D., BRUNETON, P. and CLAUER, N. 2006. Mineralogy and geochemistry of the host-rock alterations associated with the Shea Creek unconformity-type uranium deposits (Athabasca Basin, Saskatchewan, Canada). Part 1. Spatial variation of illite properties. *Clays and Clay Minerals* **54**:275-294.

POWELL, B., WOOD, G. and BZDEL, L. 2007. Advances in geophysical exploration for uranium deposits in the Athabasca Basin. In: MILKEREIT, B. (ed) *Proceedings of Exploration 07: Fifth Decennial International Conference on Mineral Exploration, Toronto, Canada, 2007*, 771-790.

ROSE, A.W., HAWKES, H.E. and WEBB, J.S. 1979. *Geochemistry in Mineral Exploration*. Academic Press, London.

SCHREINER, B. 1984. Quaternary geology of the Precambrian shield, Saskatchewan. *Saskatchewan Energy and Mines Saskatchewan Energy and Mines Report 221*.

SHILTS, W. 1995. Geochemical partitioning in till. In: BROBROWSKY, P.T., SIBBICK, S.J., NEWELL, J.M., MATYSEK, P.F. (eds) *Drift Exploration in the Canadian Cordillera, British Columbia, Ministry of Energy, Mines and Petroleum Resources*, Paper 1995-2, 149-163.

SOPUCK, V., de CARLA, A., WRAY, E. and COOPER, B. 1983. The application of lithogeochemistry in the search for unconformity-type uranium deposits, northern Saskatchewan, Canada. *Journal of Geochemical Exploration* **19**:77-99.

STEWART, P. C. 2015. The viability of surficial geochemical methods for deep unconformity-related U exploration in the Athabasca Basin, Canada. MsC thesis, Queen's University, Canada.